

1 **Reply to Comment on Franz et al. (2023): A reinterpretation of the 1.5 billion year old Volyn**
2 **'biota' of Ukraine, and discussion of the evolution of the eukaryotes, by Head et al. (2023)**

3
4 **Gerhard Franz¹, Vladimir Khomenko^{1,2}, Peter Lyckberg³, Vsevolod Chornousenko⁴, Ulrich**
5 **Struck⁵**

6 ¹Institut für Angewandte Geowissenschaften, Technische Universität Berlin, D-10587 Berlin,
7 Germany

8 ²M.P. Semenenko Institute of Geochemistry, Mineralogy and Ore Formation, The National
9 Academy of Sciences of Ukraine, 34, Palladina av., Kyiv, 03142, Ukraine

10 ³Luxembourg National Museum of Natural History, 25 Rue Münster, 2160 Luxembourg,
11 Luxembourg

12 ⁴Volyn Quartz Samotsvety Company, Khoroshiv (Volodarsk-Volynski), Ukraine*

13 ⁵Museum für Naturkunde Berlin, Invalidenstraße 43, D-10115 Berlin, Germany

14 *now at: Kondratyuka str. 9, ap. 25, Zhytomyr, 10009 Ukraine

15
16 Correspondence: Gerhard Franz (gerhard.franz@tu-berlin.de; gefra548@gmail.com)

17
18 **Abstract.** Head et al. (2023) emphasize the importance of the Volyn biota for the evolution,
19 especially in the so-called 'boring billion', in a detailed outline about the biological and
20 geological context. However, they question that the Volyn biota represent Precambrian fossils
21 and instead argue that they contain young contaminants of 'museum dust'. In addition, they
22 question their biotic origin. We present here a detailed discussion of their points of concern
23 based on presented data, including some additional information. Their points of concern
24 were:

- 25 - One object, shown by Franz et al. (2023) is similar to a pollen grain, another object is
26 similar to trichomes; we show indications for fossilization and summarize our
27 arguments against 'museum dust'.
- 28 - They question the fossil character of the biota and argue for a biomineralization; we
29 show that the biomineralization in trichomes is distinct from the mineralization of the
30 biota.
- 31 - They missed information about the internal structure; we repeat the presented
32 information about the internal structure in more detail, which is also indicative of fossil
33 material and inconsistent with trichomes.
- 34 - They argue that we did not compare via infrared spectroscopy the biota with recent
35 fungi; since the biota experienced temperatures near 300°C, we think that a
36 comparison with thermally degraded chitosan is more appropriate.
- 37 - They question the use of strongly negative $\delta^{13}\text{C}$ as an argument for biotic origin, but
38 we show that in combination with positive $\delta^{15}\text{N}$ values and the geological situation, a
39 biotic origin is more likely than abiotic synthesis.

40 In addition, Popov (2023) questioned the age of the Volyn biota, which we postulated as
41 between approximately 1.5 and 1.7 Ga. He argues that the fossils could be Phanerozoic. We
42 will also outline our arguments for the minimum age of 1.5 Ga.

43
44 **1 Introduction**

45 We thank Head et al. (2023) for stimulating the discussion about the Volyn biota. They
46 question that these are fossils, instead argue that at least some of them are young
47 contaminants by plant hairs and pollen. This could have occurred during storage as what they
48 called 'museum dust' or during sampling. Furthermore, they question the biogenicity and
49 argue for an abiotic origin. We appreciate their comment, because this question of
50 contamination was not raised before, neither in our papers from 2017, 2022, and 2023, nor in
51 any of the previous publications about kerite from Volyn.

52 **1.1 Review of kerite formation**

53 The words 'kerite' and 'kerogen' are derived from the Greek word *κηρός* (*kērós*) meaning
54 "wax". Kerogen is the insoluble residue of organic matter in sedimentary rocks that is left after
55 its treatment by common organic solvents (Durand 1980); the soluble fraction is called
56 bitumen. With increasing temperature, solid oil bitumens range from asphaltite over kerite to
57 anthraxolite; kerite (high and low) has a density of 1.05-1.3; an atomic C/(C+H+N+O) of 0.39-
58 0.62, H/C (at) of 0.59-1.44, a composition (in wt%) of 69-91 C; 4.5-9 H, 0.5-2 N, 1-12 O (Moroz
59 et al. 1998). Moroz et al. (1998) and Ciarniello et al. (2019) also considered kerite as an analog
60 for extraterrestrial organic matter.

61 Kerite from the Volyn occurrence was first described as an abiogenic material (Ginzburg
62 et al., 1987; Luk'yanova et al., 1992) and as a prime example of protein synthesis by inorganic
63 processes (Yushkin 1996). Its composition is given as (wt%) C 76.51; H 5.02; O+N 17.46; S 0.42;
64 Cl 0.24; Fe 0.06; Cu 0.15 with a chemical formula $C_{491}H_{386}O_{87}S(N)$. Among many minor
65 impurities Yushkin (1996) lists Si, Al, Na, K, and Mg, and he mentions very light isotopic $\delta^{13}C$
66 of -40 ‰. However, kerite from Volyn was later reinterpreted as fossilized cyanobacteria
67 (Gorlenko et al., 2000; Zhmur, 2003), transported in a geyser system from ponds at the surface
68 into the depth, where it is found now in cavities of pegmatitic rocks.

69

70 **1.2 Discussion points**

71 The main points of discussion are the i) possible contamination during or after sampling; ii)
72 the type of the kerite organic matter including its chemical composition and its structure; iii)
73 the morphology of the different objects, as observed under the scanning electron microscope
74 (SEM) and comparison what Head et al. (2023) described as contamination; iv) the available
75 age constraints of the fossils and further possibilities for dating; and, finally, v) a summary with
76 the open questions.

77

78 **2 Occurrence of kerite and sampling**

79 The following information is based on logbooks from the mine (VC, mine geologist in the area
80 since 1990) who also collected the material for our study together with PL. The samples of
81 kerite occur in situ underground in several, but not all shafts of the Volyn pegmatite district.
82 Within the large, miarolitic cavities ('chambers' in the original literature) kerite is also found
83 in the mineral matrix (feldspar, mica, clay minerals) on the floor of the pegmatite and is also
84 hanging from the walls or the ceiling. However, kerite in visible amounts is not preserved in
85 most chambers. It was either destroyed during cleaning and gemstone extraction, or it was
86 already collected. In those chambers which were explored by drilling, it was completely
87 destroyed by drilling fluids mixed with clay that covered the whole ground of the chambers.
88 Well-preserved large amounts of kerite were found only in new pockets opened by miners
89 underground without drilling. In January 2013 kerite was found (PL) in a 5 mm wide zone
90 around topaz crystals on the wall of a 15 m tall chamber in shaft 3. Kerite was observed
91 growing at the base of dark lilac to black fluorite crystals, in larger fiber masses around large

92 topaz crystals, as larger fiber masses in clay along the lower walls and as large masses on well
93 crystallized feldspars, mica, quartz and topaz high on the walls in two chambers.

94 Early descriptions in the drilling logbooks mention in some cases that chambers were full
95 of kerite, up to 25 kg of kerite(!) in the rather small pegmatite body from shaft 3, which has
96 accesses to several pegmatite bodies (consistent with reports in the literature, e. g. Ginzburg
97 et al., 1987). Material from this shaft was distributed to museums in the former Soviet Union.
98 The chambers are now in a depth of up to 96 m, some were mined in open pits, but the
99 crystallization depth of the pegmatites was at a depth corresponding to 2-3 kbar. Thus,
100 significant uplift had occurred since intrusion at 1.76 Ga, but there is no indication from the
101 geological literature of the area that the chambers were directly on or beneath the surface
102 and buried again later. Therefore, contamination within the chambers by plant roots going
103 down to 96 m is less likely. In any case, we have no doubt that kerite is part of the deep
104 biosphere. Most trichomes (plant hairs) are known from plants on the surface, not from deep
105 biosphere.

106 Samples kerite 1 to kerite 7 were sampled underground by PL and VC, put into firmly
107 closed plastic sample bags (double ones with label in outer one), transported first to
108 Luxemburg and then sent to Berlin. There was no need to separate kerite from the rocks and
109 from the soil, the material could be picked up. Sample bags were opened only in the electron
110 microscopy laboratory of TU Berlin, which is a special building for electron microscopy with
111 the appropriate arrangements to prevent contamination by dust. All rooms are equipped with
112 airlocks for climatization and in addition water-cooled ceilings minimizes airstream and dust
113 movement in the rooms. Samples were prepared in an exhaust hood. Of course, we cannot
114 completely rule out that some objects are contaminants, but the overwhelming majority of
115 objects on the aluminum sample holders for SEM are original as recovered from underground.
116 The only kerite sample, which could have been contaminated in a museum is our sample
117 'kerite 0'.

118 The beryl crystal sample V2008 was collected from the mine tailings in 2008 by GF, stored
119 at TU Berlin in a common wooden rock cabinet. For this sample, contamination on the mine
120 tailings or later is possible.

121 The breccia with the beryl pseudomorph was also collected from the mine tailings in 2008
122 by GF, stored at TU Berlin in a common wooden rock cabinet, and consolidated with epoxy for
123 preparation of thin sections and polished blocks for the Ar-Ar-determination of muscovite.

125 **3 Composition and structure of kerite**

126 **3.1 Organic matter in the beryl pseudomorph**

127 We start the discussion with the OM in the pseudomorph. For this, a later contamination can
128 safely be excluded, as it was discovered in thin sections. It is closely surrounded and
129 intergrown with macroscopically black, in thin section brown, C-H-bearing opal (Franz et al.
130 2017; see their fig. 6). The chemical composition of the OM is characterized by a high amount
131 of Zr, Y, Sc, and REE. These high fieldstrength elements (HFSE) are positively correlated with
132 O, and increasing O contents are correlated with decreasing C contents. The N content is
133 between 2 and 4 at%, much lower than the original kerite (see their fig. 7), which has near 8-
134 9 at% (Ginzburg et al., 1987; Yushkin, 1996). Mobilization of HFSE is possible with a F-rich fluid
135 (Loges et al. 2023), and a high F-content in the system is likely because the pegmatites
136 themselves belong to the Nb-Y-F-type and contain a high amount of topaz. In addition, the
137 muscovite in the breccia is F-rich, and fluorite is a common mineral associated with kerite (see
138 below). For further details such as transmission electron microscopy of the border zone of OM
139 to opal and about opal itself, the reader is referred to our original publication.

140 We postulated that the low N-content was caused by decay of kerite, producing NH_4 ,
141 which was responsible for K- NH_4 exchange reactions in K-feldspar and in muscovite, forming
142 buddingtonite and tobelite. There is no doubt that before the formation of the breccia and
143 the pseudomorph, OM was present in the system. Buddingtonite is not a rare mineral in the
144 Volyn pegmatite field (Proshko, 1987) and the high activity ratio for NH_4^+/K^+ required to
145 transform K-feldspar into buddingtonite (Mäder et al., 1996) indicates a large amount of
146 decayed OM. This is not consistent with Head et al.'s concern that the OM in the pegmatite
147 field is late-stage contamination. Also, the chemical composition of the OM is completely
148 incompatible with anything like museum dust or plant hairs.

149

150 **3.2 Fossil or non-fossilized OM**

151 Head et al. (2023) question the fossil character of kerite. Here we want to summarize the
152 presented information about the metamorphic, mature character of kerite.

153 After the occurrence of OM in the pegmatitic environment, the temperatures had
154 reached again approximately 300 °C (Franz et al. 2017). This estimate is based on the phase
155 equilibria with bertrandite and muscovite in the pseudomorph. Furthermore, within beryl we
156 observed fluid inclusions with C-H, which occur on cracks sealed by secondary beryl (Vozniak
157 et al., 2012). This implies that temperatures were above the lower thermal stability of beryl,
158 which is at low pressure near 300 °C (Barton and Young, 2002). These temperatures are
159 consistent with our observation on decomposition of chitin to chitosan described in detail in
160 Franz et al. (2023a), see below the discussion about FTIR data.

161 All kerite samples were investigated by open-system pyrolysis. They do not differ
162 significantly, and all spectra show characteristics of mature to very mature OM (figure 13 in
163 Franz et al. 2022, and in supplement). This excludes young contamination by plant hairs.
164 Similarly, the light microscopic investigations in cross sections with white and UV light show
165 clear indications by different reflectivity and fluorescence, not consistent with young OM. We
166 described brittle behavior of kerite, also not compatible with young unmetamorphosed OM.
167 Brittle behavior was also noted by Yushkin (1996). Luk'ynaova et al. (1982) described X-ray
168 diffraction investigations with a diffuse peak at 8° Theta indicating OM with some graphite-
169 like sheets.

170 Head et al. (2023) refer to mineralized trichomes (Mustafa et al. 2017, 2018; Ensikat et al.
171 2017) and take this as an argument against fossilization. These plant hairs are biomineralized
172 with Ca-carbonate, Ca-phosphate and silica, especially at the tip of the trichomes. This
173 biomineralization is quite different from what we interpreted as fossilized and mineralized
174 rims of the Volyn kerite. We wrote that the most conspicuous feature is the common
175 occurrence of Si-Al-O, interpreted as Al-silicates. In the quoted investigations Al was never
176 observed. Furthermore, Ca-phosphate was observed in kerite only at some places at nano-
177 sized crystals (see e.g. figure 11 in Franz et al. 2022), at variance with a continuous
178 biomineralization on the tips. Kerite is completely surrounded by a mineralized rim, whereas
179 trichomes are only mineralized at their tips. All different kerite morphologies are mineralized
180 in the same way.

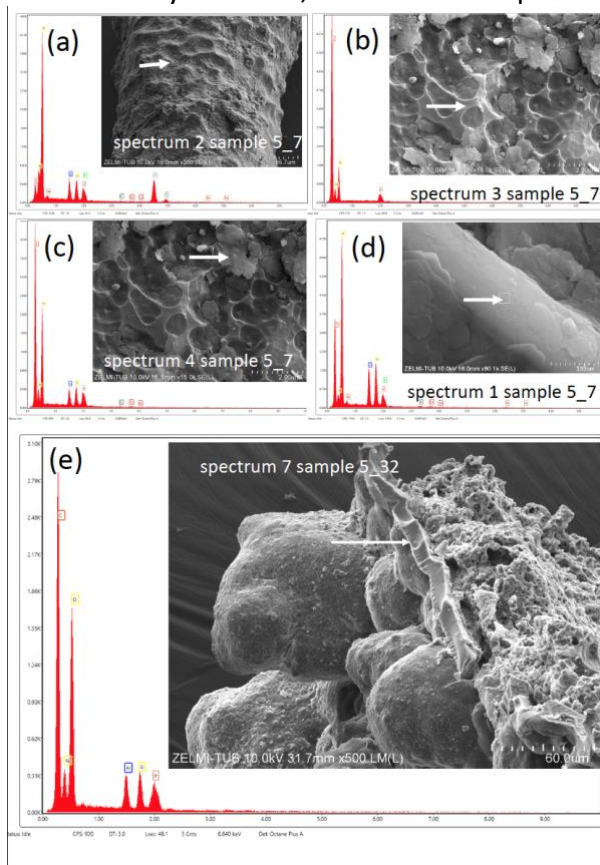
181 Concerning the analytical procedure applied by us, there is a misunderstanding in Head
182 et al.'s (2023) comment. On line 146 to 149 they wrote: "Had Franz et al. (2023) used EDX in
183 addition to applying EDAX EDS to selected cross sections, they would have been easily able to
184 determine the elemental distribution for all specimens they imaged using SEM which could
185 have assisted in discriminating extant contaminations from fossil material." For our element
186 mapping we used wave length dispersive (WDS) analysis with the electron microprobe (EMP),
187 which is much more sensitive than energy dispersive systems (EDS) such as EDAX. We have

188 shown several element distribution maps of different morphologies in Franz et al. (2022), and
189 since all show generally identical features with an Al-Si-Ca rim structure and an internal
190 structure with characteristic N-O-S distribution, we can safely exclude biomineralization, but
191 instead mineralization due to a fossilization process.

192

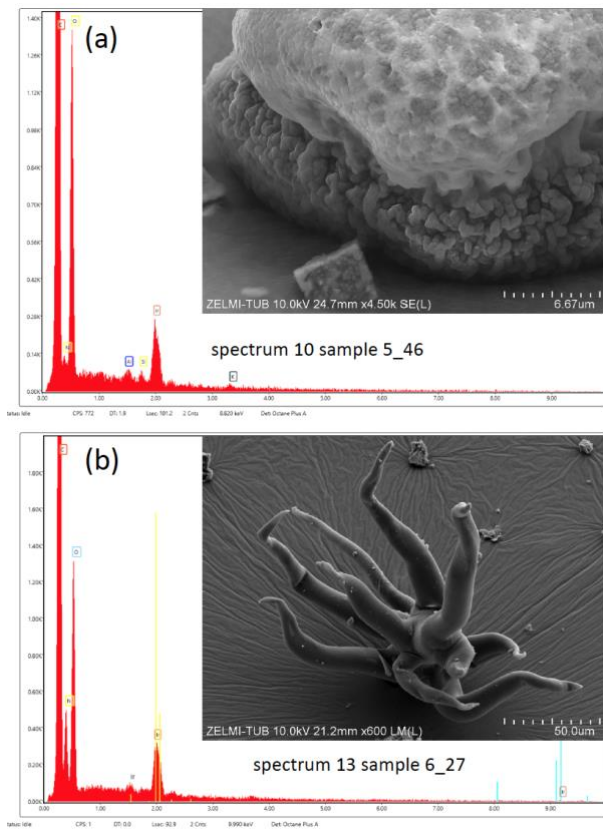
193 3.3 EDS (with SEM)

194 All spectra of kerite objects show a high amount of oxygen. This excludes fresh organisms but
195 indicates again (highly) mature OM. Minerals on the surface of filamentous kerite (Fig. 1a-d),
196 of bulbous kerite (Fig. 1e), and of the spherical object, interpreted by Head et al. (2023) as a
197 pollen, are mostly Al-silicates, some with K, Na, and Ca. The flaky shape of the minerals
198 indicates clay minerals, one needle-shaped crystal is a Ti-oxide, possibly rutile.

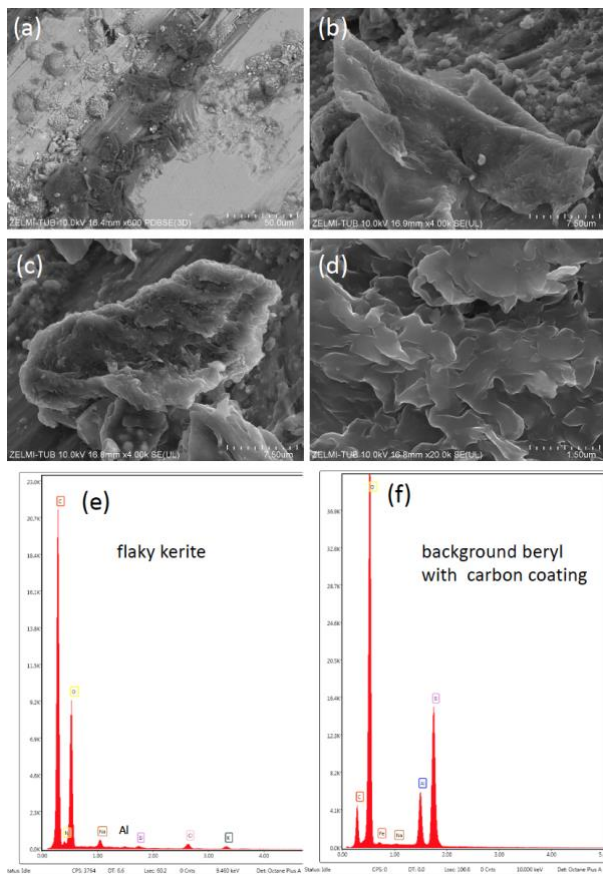


199

200 **Figure 1.** EDS spectra obtained with the SEM of filamentous (a, b, c, d) and bulbous (e) kerite
201 objects. (a) Needle-shaped small object with high Ti-O contents (arrow; interpreted as rutile)
202 next to Al-silicates with minor amounts of Na, K, and Ca. (b) Spectrum of clear surface (arrow)
203 of kerite, showing only the kerite composition of C-N-O. (c) Spectrum of platy mineral grains
204 (arrow) with Al-Si and small contents of K and Fe, interpreted as a clay mineral. (e) Base
205 (arrow) of bulbous kerite, with high amounts of Al-Si. Samples are iridium-coated.

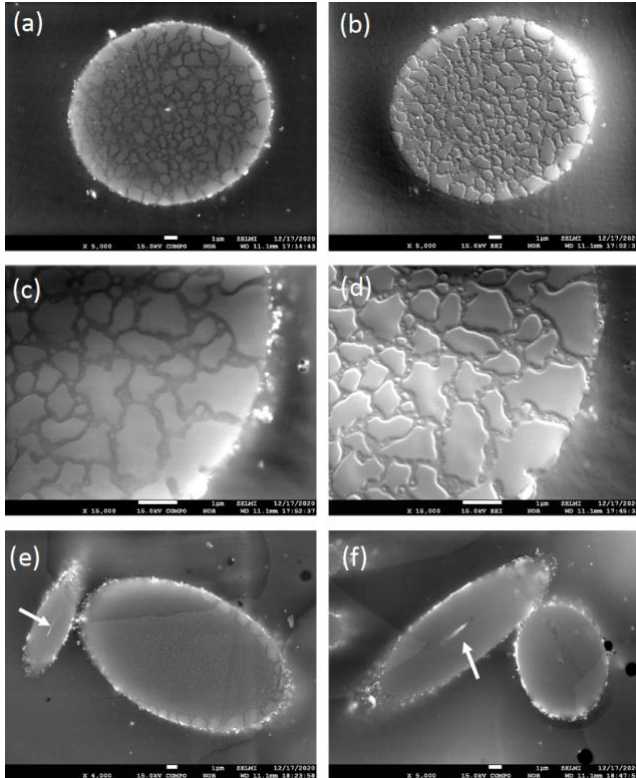


206
 207 **Figure 2.** EDS spectra of a spherical object (a) and a filamentous object (b). The spherical object
 208 shows Al-Si-K peaks, which can be interpreted as illite, whereas the filamentous object shows
 209 only the typical composition of kerite with C-N-O; both samples are iridium-coated.
 210



211

212 **Figure 3.** EDS data of flaky kerite, observed on sample V2008, a beryl crystal. (a, b, c, d) show
 213 the structure of kerite, in (a) with combined BSE detector for element contrast. The dark
 214 contrast compared to background beryl and other minerals indicates low average atomic
 215 number. (e) is the corresponding EDS spectrum with clear indication for Si, Al, Na, K, and Cl,
 216 next to C-N-O of kerite. (f) is EDS spectrum of beryl; note the low C-peak caused by carbon
 217 coating, compared to the large C-peak of kerite.
 218



219 **Figure 4.** BSE (a, c, d, e) and SE (b, d) of cross sections of filamentous kerite, embedded in
 220 epoxy. Note the discontinuous rim of high contrast indicating mineralized parts, and within
 221 the channel (e, f) also with high contrast (arrows). The mosaic pattern with different contrast
 222 in BSE (a, c) is seen in SE images (b, d) as slightly lower areas of approximately 200 nm width.
 223
 224

225 The EDS spectrum of the object, interpreted as pollen by Head et al. (2023), also shows
 226 the presence of Al and Si, together with the typical C-N-O peaks (Fig. 2). The EDS spectrum of
 227 the object, interpreted by Head et al. (2023) as trichome 'museum dust' (Fig. 3) shows no Al-
 228 Si, but the C-N-O ratios are very similar to those of the mineralized filaments, and therefore
 229 we have no doubts that this is also fossilized OM.
 230

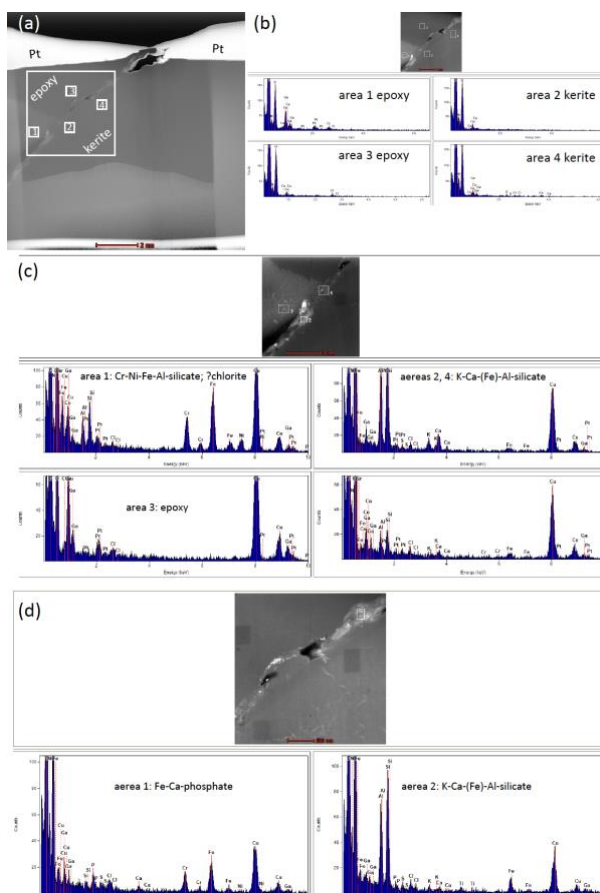
231 3.4 EMPA data

232 In BSE images of cross sections of filamentous kerite we see a discontinuous mineralized rim
 233 (Fig. 4). In combination with the element mappings (see images in figures 8 to 11 in Franz et
 234 al. 2022, and figures S6, S7 in the supplement to Franz et al. 2022), we can safely conclude
 235 that the mineralized rim consists dominantly of Al-silicates. Some other minerals such as Ca-
 236 phosphate or silica occur only in isolated spots and do not cover the whole rim. Over a distance
 237 of approximately 1 μm the filament shows a higher contrast rim in BSE images, indicating a
 238 higher average atomic number, consistent with our interpretation that this is caused by a
 239 mineralized, impregnated rim of dominantly Al-silicates. In the internal structure of the
 240 filament, a mosaic pattern can be observed with approximately 200 nm wide channels, also

241 indicated by different element contrast (Fig. 4a, b). In SE images (Fig. 4c, d) a slightly lower
242 position of the channels is seen, caused by different behavior during polishing. This internal
243 structure is compatible with fossilized material, not with fresh cells of trichomes.
244

245 3.5 TEM data

246 In addition to the TEM investigations we presented in Franz et al. (2017), we cut a new focused
247 ion beam (FIB) foil from a filamentous object (Fig. 5). The foil covers the embedding material
248 epoxy (characterized by typical Cl-content), the approximately 500 nm wide rim and kerite
249 (with dominantly C-O and N). The rim consists of a mixture of different minerals, which can be
250 distinguished by different contrast in the HAADF images. EDAX spectra indicate dominantly
251 Al-silicates with minor amounts of K, Ca, and Fe, and Fe-Ca-phosphate. This is different from
252 the type of biomineralization in trichomes, shown by Mustafa et al. (2017, 2018) and Ensikat
253 et al. (2017).
254



255 **Figure 5.** Analytical EDAX-TEM results on a FIB from the rim of a filamentous kerite object.
256 Note for all spectra that Ga-peaks are due to the Ga ion cutting, Cu peaks originate from the
257 copper grid, and Pt from the platinum holder. (a) Overview of the FIB foil; white frame
258 indicates position of (b) high-angular annular dark-field (HAADF) image and EDAX spectra of
259 kerite and embedding material epoxy. (c) Detail of (b) with EDAX spectra of three inclusions,
260 interpreted as possibly chlorite and a complex Al-silicate, possibly a clay mineral. (d) Detail of
261 (b) with EDAX spectra of two inclusions, a Fe-Ca-phosphate and a complex Al-silicate.
262

263 3.6 IR spectra

264 Head et al. (2023) criticize our IR spectra and argue that we should have used modern fungal
265 chitin standards for comparison and a more detailed comparison with sub-fossil and fossil
266 fungi. Since we knew that the Volyn biota experienced temperatures near 300 °C, comparison
267

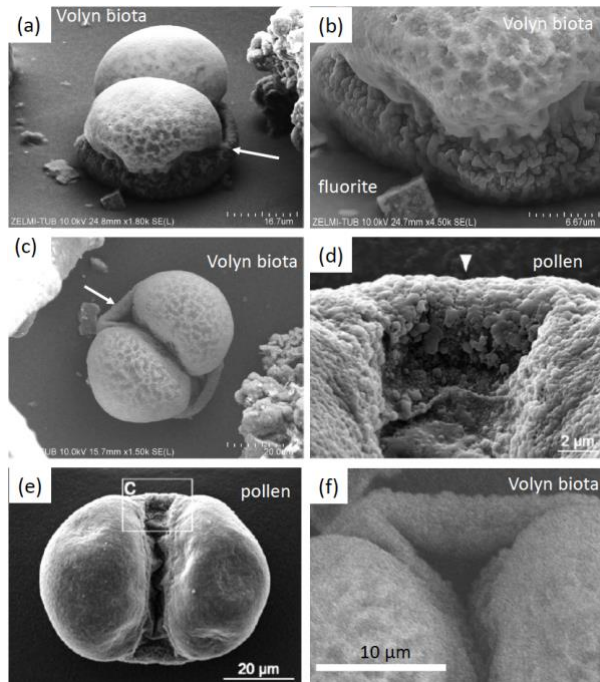
268 with modern fungi did not seem appropriate to us. Instead, we followed the procedure by
269 Loron et al. (2019) and the thermal degradation studies of chitosan (Wanjun et al., 2005;
270 Zawadzki and Kaczmarek, 2010; Vasilev et al., 2019). These are clearly consistent with our
271 conclusion that chitosan is a constituent of the kerite material.

272

273 **4 Comparison of kerite morphology**

274 Head et al. (2023) present evidence for strong similarity of one object of our sample collection
275 with pollen of an extinct conifer. The similarity is indeed striking, but we want to stress
276 important differences (Fig. 6):

277



278

279 **Figure 6.** SEM images for direct comparison of kerite object from Volyn biota (a, b, c, f) and
280 *Pinus* pollen (d, e) from Head et al. (2023). Note that the kerite object is sitting firmly on base
281 consisting of OM (a, b), whereas pollen are free objects. The surface of kerite is characterized
282 by dents (b), whereas the pollen shows a microrogulate surface (d). What is described from
283 pollen as air sacs (d, e) sits on a similar height as the pollen grain itself (d), whereas what we
284 described as a sheath comes from the base of the kerite object (arrows in a and c). This sheath
285 shows some inward folding (f), which is not seen in the air sac of the pollen.

286

287 The kerite object is sitting firmly on a base consisting of OM (Fig. 6a, b), whereas pollen
288 are free objects. The surface of kerite is characterized by dents (Fig. b), whereas the pollen
289 shows a microrogulate surface (Fig. d). What is described from pollen as air sacs (Fig. 6d, e)
290 sits on a similar height as the pollen grain itself, whereas what we described as a sheath comes
291 from the base of the kerite object (arrows in Fig. 6a, c). This sheath shows some inward folding
292 (Fig. 6f), which is not seen in the air sac of the pollen.

293

294 The other object, which Head et al. (2023) interpret as a plant hair (figure 3 j, k, l; in Franz
295 et al. 2023a) due to the similarity to ‘museum dust’, also sits firmly on a base. If such a delicate
296 object like unfossilized trichomes was transported down into the chamber (where it was
297 sampled), it is difficult to imagine that it survived the transport.

298

299 Head et al. (2023) restrict their criticism to these two objects but do not mention the fact
that the large majority of objects we presented has a different morphology, with filaments up
to the mm-size, bulbous objects, objects with irregular shape etc. None of these objects is

300 similar to trichomes. Also, they do not mention the internal structure with a channel, which
301 we documented in detail (figure 11 in Franz et al., 2023a), and which is obvious also in BSE
302 images (Fig. 4). They also do not mention the presence of Bi(Te,S) biomineralization, which we
303 documented (figure 10 in Franz et al., 2023). To the best of our knowledge, this type of
304 biomineralization was not observed in trichomes.

305

306 **5 Age of the fossils**

307 Popov (2023) questioned the minimum age of the organic matter, which we proposed as 1.5
308 Ga, based on the Ar-Ar laser ablation data (Franz et al., 2022a) of muscovite in a pseudomorph
309 after beryl. He proposed a sequence of events, starting with the intrusion of the granites and
310 the pegmatites at approximately 1.76 Ga (Shumlyanskyy et al., 2017, 2021), cooling and
311 pseudomorph formation due to a hydrothermal event at 1.5 Ga, then again cooling,
312 introduction of organic matter, then a second hydrothermal event, which converted
313 muscovite into tobelite and K-feldspar into buddingtonite. The age of the second event could
314 have been early Phanerozoic, based on our data (Franz et al., 2022b) of dating attempts of the
315 kerite itself, which produced in Popov's (2023) wording an isochrone of 493 ± 98 (1s) Ma, but
316 which we considered only as a reference line due to the large uncertainty. In this sequence of
317 events the breccia formation is missing, but this event is important: It fractionated feldspar
318 and quartz into cm-sized, irregular pieces, including a large piece of pegmatitic beryl. This
319 event must have occurred before the pseudomorph formation, because the delicate
320 pseudomorph, consisting of a rather loose framework of muscovite and bertrandite would not
321 have survived the brecciation. But the breccia is cemented by black opal (pigmented by
322 hydrocarbons), and OM must have been present before precipitation of opal. Therefore, the
323 sequence of events after the intrusion must have been: Presence of organic matter,
324 brecciation, pseudomorph formation at 1.5 Ga in one event, first with muscovite formation,
325 then during decay of the kerite and production of NH_4^+ tobelite and buddingtonite (including
326 formation of secondary, C-H bearing fluid inclusions in low-T beryl), then further cooling. It
327 was made clear in our text that "...the fluid composition changed during the pseudomorph
328 formation, starting with F-dominated K-rich fluids producing pure F-muscovite, followed by
329 alternating NH_4 -rich and K-rich compositions, producing oscillatory growth zones in
330 buddingtonite (Fig. 5e) and ending with a late K-rich fluid (producing some outer K-rich zones
331 in buddingtonite; Fig. 5d)." This is the same conclusion as in our first analysis of the
332 pseudomorph's texture (Franz et al., 2017) and clear from the summary figure 13, illustrating
333 the sequence of processes in one single geological event. We feel misinterpreted by Popov
334 (2023), who wrote that in our second study we had changed our mind.

335 There might have been additional hydrothermal events since 1.5 Ga, caused e. g. by the
336 Neoproterozoic Volyn Large Igneous Province at approximately 600 Ma or later Devonian
337 rifting of the Prypyat aulacogen (Shumlyanskyy et al., 2016), but none of these events is
338 documented up to now in the pegmatites of the Volyn field. We fully agree with Popov (2023)
339 that the late-stage development of pegmatites including later overprinting by hydrothermal
340 events may point to a protracted history. However, for the Volyn locality, the late-stage
341 development is documented in Lazarenko et al. (1973) and in a study of dissolution of Volyn
342 beryl crystals with the formation of typical and diagnostic etching (Franz et al., 2023b).

343

344 **6 Origin of kerite - biotic or abiotic**

345 Head et al. (2023) conclude their discussion with "We have doubts whether any of the in-situ
346 Volyn 'biota' is organic in origin", based on references to the low $\delta^{13}\text{C}$ values obtained via
347 experiments with Fischer-Tropsch-type synthesis (FTT) under hydrothermal conditions in the

348 presence of metallic Fe. From a starting composition with an assumed value for $\delta^{13}\text{C}$ of -20 ‰,
349 different organic compounds were obtained with a rather uniform composition of -50 ‰
350 (McCollum and Seewald, 2006). Abiotic synthesis of nitrogen-bearing organic carbon species,
351 such as amino acids, is thermodynamically favored by molecular H_2 , which is produced by
352 serpentinization of Fe-rich mantle-derived rocks (Ménez et al., 2018). The presence of Fe-rich
353 minerals as catalyst for the production of abiotic carbonaceous material in serpentinites (Nan
354 et al., 2021) is not a good analogue for the granitic environment, in which Fe-rich minerals are
355 generally scarce. An FTT process is unlikely in the current geological setting of an Fe-poor
356 granite-pegmatite system.

357 Source of carbon for abiotic synthesis in Volyn should be the mantle with a uniform $\delta^{13}\text{C}$
358 value of -5 ‰ (Marty et al., 2013, and references therein), because the Korosten pluton is
359 comprised mainly of mantle-derived granitic, gabbroic, and anorthositic rocks (Shumlyansky
360 et al., 2017, 2021). Assuming a similar fractionation of -30 ‰ for a source with $\delta^{13}\text{C}$ of -5 ‰,
361 a composition of abiotic kerite should have values of -35 ‰, but many kerite bulk samples
362 have much lower values between -40‰ and -48‰. According to the model of abiotic origin,
363 mantle-derived fluids should also be the source for nitrogen. The N-isotopic signature of the
364 mantle scatters from -25 ‰ to +15, with most values around -5 ± 3 ‰ Cartigny (2005),
365 therefore a mantle source is less likely for the Volyn locale, with positive $\delta^{15}\text{N}$ values up to 10
366 ‰ throughout. A more detailed description of isotopic composition of the kerite organic
367 matter might be possible by in-situ methods. Such methods are currently not available for us,
368 but we will explore the possibility for cooperation with other laboratories.

369 An alternative source might be the country rocks of the Korosten pluton, but this would
370 require large amounts of C- and N-rich fluids, and there is no geological evidence for such
371 fluid-rock interactions. They should have left their signature also within the granites, which
372 are the hosts of the pegmatites. Yushkin (1996) presented analyses of different proteins in
373 kerite and used it as an argument that abiotic synthesis is possible. However, he starts from
374 the assumption of abiotic origin and did not consider the possibility of fossil material. The
375 large amounts of kerite of several kg recovered from the mine (Ginzburg et al., 1987) is in our
376 view more consistent with biomass accumulation; what has been described as abiotic
377 formation of carbonaceous material was observed in small amounts in thin section only (e. g.
378 Nan et al., 2021; Ménez et al., 2018).

379

380 **Summary and open questions**

381 Although the morphology of two objects, selected by Head et al. (2023) show a striking
382 similarity to recent organisms, the combination of all observations is much more in favor of
383 fossil organisms: The occurrence in the mine as part of the deep biosphere; a large variety of
384 morphologically different objects, which however have all the same type of rim
385 mineralization; their brittle behavior; the internal structure with a channel in the filaments;
386 the presence of biomineral inclusions of $\text{Bi}(\text{Te},\text{S})$.

387 Further studies on the molecular composition, i. e. certain biomarkers, will help to
388 characterize kerite in more detail and give information about the type of organisms, which
389 requires, however, more material. This is under the current situation in Ukraine not available.

390 We are aware that our single age determination of 1.5 Ga for the hydrothermal
391 overprinting of the pegmatites should be verified or falsified by ages on different minerals
392 and/or different isotope systems. If more and better data will be available, we are happy to
393 change the interpretation, but with the current available data the presented interpretation

394 seems to be the best one. We are currently working on Rb-Sr data with the laser-ablation
395 system from the same sample, which was determined by Ar-Ar and which can be applied to
396 both minerals, muscovite and feldspar. Additional sample material with white mica and
397 feldspar is also available and will be studied.

398 Fluid inclusion studies might further help to clarify the origin of kerite (Vozniak et al.,
399 2012, and references therein; Kalyuzhnyi et al., 1971). Liu et al. (2022) observed whewellite
400 ($\text{CaC}_2\text{O}_4 \cdot \text{H}_2\text{O}$) in $\text{CO}_2\text{-N}_2\text{-CH}_4$ -vapor of fluid inclusions in topaz, thought as a product of
401 oxidation of organic material with an alkaline fluid. In-situ determination of C- and N-isotopes,
402 and possibly also other stable isotopes (e.g. O, S) might also help to further clarify the type of
403 organisms, their internal structure, and their origin.

404

405

406 *Data availability.* All data are as figures in the text or in the cited references.

407

408 *Supplement.* There is no supplement to this article.

409

410 Author contributions. GF concept, figures, and writing; VK writing, FTIR; VC and PL information
411 about the sampling and occurrence.

412

413 *Competing interests.* The authors declared that they have no competing interests.

414

415 *Acknowledgements.* We thank Anja Schreiber and Richard Wirth for permission to use
416 unpublished TEM data.

417

418 *Financial support.* VK acknowledges funding by Alexander von Humboldt foundation.

419

420 **References**

421

422 Barton, M. D., and Young, S.: Non-pegmatitic deposits of beryllium: Mineralogy, geology,
423 phase equilibria and origin. *Rev. Mineral. Geochem.*, 50, 591-691, 2002.

424 Cartigny, P., Stable isotopes and the origin of diamond, *Elements*, 1, 79-84, 2005.

425 Ciarniello, M., Moroz, L. V., Poch, O., Vinogradoff, V., Beck, P., Rousseau, B., Istiqomah, I.,
426 Sultana, R., Raponi, A., Schroeder, S., Kappel, D., Quirico, E., Filacchione, G., Pommerol, A.,
427 Mennella, V., and Pilorget, C.: VIS-IR spectroscopy of mixtures of ice, organic matter and
428 opaque minerals in support of minor bodies remote sensing observations, *EPSC Abstracts* 13,
429 1467-1468, 2019.

430 Durand, B.: Sedimentary organic matter and kerogen. Definition and qualitative importance
431 of kerogen, in *Kerogen—Insoluble Organic Matter from Sedimentary Rocks* (B. Durand, Ed.),
432 pp. 13–34, Editions Technip, Paris, 1980.

433 Ensikat, H.-J., Mustafa, A., and Weigend, M.: Complex patterns of multiple biomineralization
434 in single-celled plant trichomes of the Loasaceae, *Amer. J. Botany*, 104, 195-206, 2017.

435 Franz, G. Khomenko, V. Vishnyevskyy, A. Wirth, R. Nissen, and J. Rocholl, A.: Biologically
436 mediated crystallization of buddingtonite in the Paleoproterozoic: Organic-igneous
437 interactions from the Volyn pegmatite, Ukraine, *Amer. Mineral.* 102, 2119-2135, 2017.

438 Franz, G., Sudo, M., and Khomenko, V.: $^{40}\text{Ar}/^{39}\text{Ar}$ dating of a hydrothermal pegmatitic
439 buddingtonite-muscovite assemblage from Volyn, Ukraine, *Eur. J. Mineral.*, 34, 7-18.
440 doi.org/10.5194/ejm-34-7-2022, 2022a.

441 Franz, G., Lyckberg, P., Khomenko, V., Chournousenko, V., Schulz, H.-M., Mahlstedt, N., Wirth,
442 R., Glodny, J., Gernert, U., and Nissen, J.: Fossilization of Precambrian organic matter (kerite)
443 from the Volyn pegmatite, Ukraine, *BioGeosciences*, 19, 1795-1811, 2022b.

444 Franz, G., Khomenko, V., Lyckberg, P., Chornousenko, V., Struck, U., Wirth, R., Gernert, U., and
445 Nissen, J.: The Volyn biota (Ukraine) – indications for 1.5 Gyr old eucaryotes in 3D-
446 preservation, a spotlight on the ‘boring billion’, *BioGeosciences*, 20, 1901-1924,
447 doi.org/10.5194/bg-20-1901-2023, 2023a.

448 Franz, G., Vyschnevskiy, O. A., Khomenko, V. M., Lyckberg, P., and Gernert, U.: Etch pits in
449 heliodor and green beryl from the Volyn pegmatites, Northwest Ukraine: A diagnostic feature,
450 *Gems & Gemology*, 59(3) 324-339, doi.org/10.5741/GEM;S.59.3.324, 2023b.

451 Ginzburg, A.I., Bulgakov, V.S., Vasilishin, I.S., Luk’yanova, V.T., Solntseva, L.S., Urmenova, A.M.,
452 and Uspenskaya, V.A.: Kerite from pegmatites of Volyn, *Dokl. Akad. Nauk SSSR*, 292, 188–191,
453 1987 (in Russian).

454 Gorlenko, V.M., Zhmur, S.I., Duda, V.I., Osipov, G.A., Suzina, N.E., and Dmitriev, V. V.: Fine
455 structure of fossilized bacteria in Volyn kerite, *Orig. Life Evol. Biosph.*, 30, 567–577, 2000.

456 Head, M. J., Riding, J. B., O’Keefe, J. M. K., Jeiter, J., and Gravendyck, J.: Comment on Franz et
457 al. 2023: A reinterpretation of the 1.5 billion year old Volyn ‘biota’ of Ukraine, and discussion
458 on the evolution of eucaryotes, *BioGeosciences*,
459 <https://egusphere.copernicus.org/preprints/2023/egusphere-2023-2748/>, 2023.

460 Kalyuzhnyi V. A., Voznyak, D. K., and Gigashvili, G. M.: Mineral-forming fluids and mineral
461 paragenesis of chamber pegmatites of Ukraine, Kyiv: Naukova Dumka, 216 pp., 1971 (in
462 Ukrainian).

463 Lazarenko, E. K., Pavlishin, V. J., Latysh, V. T., and Sorokon, Ju. G.: Mineralogy and genesis of
464 the chamber pegmatites from Volyn, (in Russian) Lvov, Vysskaja shkola, 360 pp, 1973.

465 Liu, Y., Schmidt, C., and Li, J.: Peralkalinity in peraluminous granitic pegmatites. I. Evidence
466 from whewellite and hydrogen carbonate in fluid inclusions, *Amer. Mineral*, 107, 233-238,
467 2022.

468 Loges, A., Manni, M., Louvel, M., Wilke, M., Jahn, S., Welter, E., Borchert, M., Qiao, S., Klemme,
469 S., and Keller, B. G.: Complexation of Zr and Hf in fluoride-rich hydrothermal aqueous fluids
470 and its significance for high field strength element fractionation, *Geochim. Cosmochim. Acta*,
471 366, 167-181, doi.org/10.1016/j.gca.2023.12.013, 2023.

472 Loron, C. C., François, C., Rainbird, R. H., Turner, E. C., Borensztajn, S., and Javaux, E. J.: Early
473 fungi from the Proterozoic era in Arctic Canada, *Nature* 570.7760: 232-235, 2019.

474 Lu'kyanova, V. T., Lobzova, R. V., and Popov, V. T.: Filaceous kerite in pegmatites of Volyn,
475 *Izvestiya Ross. Akademii Nauk Ser. Geologicheskaya*, 5, 102-118, 1992 (in Russian).

476 Mäder, U. K., Ramseyer, K., Daniels, E. J., and Althaus, E.: Gibbs free energy of buddingtonite
477 (NH₄AlSi₃O₈) extrapolated from experiments and comparison to natural occurrences and
478 polyedral estimation, *Eur. J. Mineral.*, 8, 755-766, 1996.

479 Marty, B., Alexander, O’D., and Raymond, S. N.: Primordial origins of Earth’s carbon. *Reviews*
480 *Mineral. Geochem.*, 75, 149-181, 2013.

481 McCollom, T. M., and Seewald, J. S.: Carbon isotope composition of organic compounds
482 produced by abiotic synthesis under hydrothermal conditions, *Earth Planet. Sci. Lett.*, 243,
483 74-84, doi.org/10.1016/j.epsl.2006.01.027, 2006.

484 Ménez, B., Pisapia, C., Andreani, M., Jamme, F., Vanbellinghen, Q., et al.: abiotic synthesis of
485 amino acids in the recesses of the oceanic lithosphere, *Nature*, 564 (7734), 59-63,
486 doi.org/10.1038/s41596-018-0684-z.hal-02111638, 2018.

487 Moroz, L. V., Arnold, G., Korochantsev, A. V., and Wäsch, R.: Natural solid bitumens as possible
488 analogs for cometary and asteroid organics: 1. Reflectance spectroscopy of pure bitumens,

489 ICARUS 134: 253-268, 1998.
490 Mustafa, A., Ensikat, H.-J., and Weigend, M.: Ontogeny and the process of biomineralization
491 in the trichomes of Laocaceae, *Amer. J. Botany*, 104(3), 367-378, 2017.
492 Mustafa, A., Ensikat, H.-J., and Weigend, M.: Mineralized trichomes in Boraginales: complex
493 microscale heterogeneity and simple phylogenetic patterns, *Ann. Botany*, 121, 741-751, doi:
494 10.1093/aob/mcx191, 2018.
495 Nan, J., King, H. E., Delen, G., Meirer, F., Weckhuysen, B. M. Guo, Z., Peng, Z., and Plümper,
496 O.: The nanogeochemistry of abiotic carbonaceous matter in serpentinites from the Yap
497 Trench, western Pacific Ocean, *Geology*, 49, 330-334, doi.org/10.1130/G48153.1, 2021.
498 Popov, D. V.: Do pegmatites crystallise fast? A perspective from petrologically-constrained
499 isotopic dating, *Geosciences*, 13, 297, doi.org/10.3390/geosciences13100297, 2023.
500 Proshko, V. Ya., Bagmut, N. N., Vasilishin, I. S., and Panchenko, V. I.: Ammonium feldspars from
501 Volyn pegmatites and their radiospectroscopic properties, *Mineral. J. (Ukraine)*, 9, 67-71, 1987
502 (in Russian).
503 Shumlyansky, L., Nosova, A., Billström, K., Söderlund, U., Andréasson, P.-G., and
504 Kuzmenkova, O.: The U–Pb zircon and baddeleyite ages of the Neoproterozoic Volyn Large
505 Igneous Province: implication for the age of the magmatism and the nature of a crustal
506 contaminant, *Gff-Upsala*, 138(1), 17-30, 2016.
507 Shumlyansky L., Hawkesworth C., Billström K., Bogdanova S., Mytrokhyn O., Romer R.,
508 Dhuime B., Claesson S., Ernst R., Whitehouse M., and Bilan O.: The origin of the
509 Palaeoproterozoic AMCG complexes in the Ukrainian Shield: new U-Pb ages and Hf isotopes
510 in zircon. *Precam. Res.*, 292, 216-239, 2017.
511 Shumlyansky, L., Franz, G., Glynn, S., Mytrokhyn, O., Voznyak, D., and Bilan O.:
512 Geochronology of granites of the western part of the Korosten AMCG complex (Ukrainian
513 Shield): implications for the emplacement history and origin of miarolitic pegmatites, *Eur. J.*
514 *Min.*, 33, 703-716, 2021.
515 Vasilev, A., Efimov, M., Bondarenko, G., Kozlov, V., Dzidziguri, E., and Karpacheva, G.: Thermal
516 behavior of chitosan as a carbon material precursor under IR radiation, *IOP Conf. Ser.: Mater.*
517 *Sci. Eng.*, 693, 2019. doi.org/10.1088/1757-899X/693/1/012002.
518 Voznyak, D.K., Khomenko, V.M., Franz, G., and Wiedenbeck, M.: Physico-chemical conditions
519 of the late stage of Volyn pegmatite evolution: Fluid inclusions in beryl studied by
520 thermobarometry and IR-spectroscopy methods, *Mineral. J. (Ukraine)*, 34, 26–38, 2012 (in
521 Ukrainian).
522 Wanjun T., Cunxin W., and Donghua, C.: Kinetic studies on the pyrolysis of chitin and chitosan,
523 *Polym. Degrad. Stabil.*, 87, 389–394, 2005.
524 Yushkin, N. P.: Natural polymer crystals of hydrocarbons as models of prebiological organisms,
525 *J. Crystal Growth*, no. 167, 237-247, 1996.
526 Zawadzki, J., and Kaczmarek, H.: Thermal treatment of chitosan in various conditions,
527 *Carbohydr. Polym.*, 80, 394-400, 2010.
528 Zhmur, S. I.: Origin of Cambrian fibrous kerites of the Volyn region, *Lithol. Mineral Resour.*, 38,
529 55-73, 2003.